18

Doppler Radar Tracking Using Moments

Mohammad Hossein Gholizadeh and Hamidreza Amindavar
Amirkabir University of Technology, Tehran
Iran

1. Introduction

A Doppler radar is a specialized radar that makes use of the Doppler effect to estimate targets velocity. It does this by beaming a microwave signal towards a desired target and listening for its reflection, then analyzing how the frequency of the returned signal has been altered by the object's motion. This variation gives direct and highly accurate measurements of the radial component of a target's velocity relative to the radar. Doppler radars are used in aviation, sounding satellites, meteorology, police speed guns, radiology, and bistatic radar (surface to air missile).

Partly because of its common use by television meteorologists in on-air weather reporting, the specific term "Doppler Radar" has erroneously become popularly synonymous with the type of radar used in meteorology.

The Doppler effect is the difference between the observed frequency and the emitted frequency of a wave for an observer moving relative to the source of the waves. It is commonly heard when a vehicle sounding a siren approaches, passes and recedes from an observer. The received frequency is higher (compared to the emitted frequency) during the approach, it is identical at the instant of passing by, and it is lower during the recession. This variation of frequency also depends on the direction the wave source is moving with respect to the observer; it is maximum when the source is moving directly toward or away from the observer and diminishes with increasing angle between the direction of motion and the direction of the waves, until when the source is moving at right angles to the observer, there is no shift. Since with electromagnetic radiation like microwaves frequency is inversely proportional to wavelength, the wavelength of the waves is also affected. Thus, the relative difference in velocity between a source and an observer is what gives rise to the Doppler effect.

Now, suppose that we have received an unknown waveform from the target. This waveform is a result of reflection from a fluctuating target in presence of clutter and noise. The received signal is often modeled as delayed and Doppler-shifted version of the transmitted signal. So not only the Doppler estimation, but the joint estimation of the time delay and Doppler shift provides information about the position and velocity of the target. So we should focus on the joint estimation of both parameters. There are many works for estimating the joint time delay and Doppler shift, with advantages and disadvantages apiece. Among these methods, Wigner Ville (WV) method has proven to be a valuable tool in estimating the time delay and Doppler shift. WV method is a time-frequency processing. It possesses a high resolution in the time-frequency plane and satisfies a large number of desirable theoretical properties [Chassande-Mottin & Pai, 2005]. In fact, these properties are the fundamental motivation

for the use of the narrowband(wideband) WV transformation for detecting a deterministic signal with unknown delay-Doppler(-scale) parameters. WV's practical usage is limited by the presence of non-negligible cross-terms, resulting from interactions between signal components. Alternative approaches are proposed for eliminating or at least suppressing the cross-terms [Chassande-Mottin & Pai, 2005; Orr et al., 1992; Tan & Sha'ameri, 2008]. Generally speaking, cross-term suppression may be divided into two categories: signal-independent and signal-dependent paradigm. Coupling the Gabor transformation with the WV distribution is a signal-independent procedure that reveals a cross-term suppression approach through exploitation of partial knowledge about signals to be encountered [Orr et al., 1992]. For signal-dependent method, it is possible to apply an adaptive window over WV distribution where the kernel parameters are determined automatically from the parameters of the input signal. This kernel is capable of suppressing the cross-terms and maintain accurate time-frequency resolution [Tan & Sha'ameri, 2008]. Besides the WV method, there are other time-frequency techniques such as wavelet transform. Wavelet approach combines the noise filtering and scaling together, yielding a reduction in complexity [Niu et al., 1999]. There is also another procedure using the fractional lower order ambiguity function (FLOAF) for joint time delay and Doppler estimation [Ma & Nikias, 1996]. Now another view is presented. It is assumed that the transmitted signal follows an N-mode Gaussian mixture model (GMM). GMM can be used for different transmitted signals. Especially, it presents an accurate modeling for actual signals transmitted in the sonar and radar systems [Bilik et al., 2006]. The received signal is affected by the noise, time delay and Doppler where the conglomerate effects on the signal cause peculiar changes on the moments of received signal. Using moments is a powerful procedure which is used for different applications, specially in parameter estimation. Some people use the moment method to estimate the parameters of a Gaussian mixture in an environment without noise [Fukunaga et al., 1983]. Some apply the method for better parameter estimation in a faded signal transmitted through a communication channel which is suffered from multipath. The method can be implemented using a non-linear least-squares algorithm to represent a parameterized fading model for the instantaneous received path power which accounts for both wide-sense stationary shadowing and small-scale fading [Bouchereau & Brady, 2008]. The most prominent and novel models for the envelope of a faded signal are Rician and Nakagami. There are estimators for the Nakagami-m parameter based on real sample moments. The estimators present an asymptotic expansion which provides a generalized closed-form expression for the Nakagami-m parameter without the need for coefficient optimization for different ratios of real moments [Gaeddert & Annamalai, 2005]. There are also approaches that show the K-factor in Rician model is an exact function of moments estimated from time-series data [Greenstein et al., 1999].

In this chapter, we analyze the effect of noise, time delay, and Doppler on the moments of received signal and exploit them for estimating the position and velocity of the target. We note that in the new method, the noise power is assumed unknown which is estimated along with the time delay and Doppler shift. The new approach exhibits accurate results compared to the existing methods even in very low SNR and long tailed noise. Then, the estimated parameters are used for tracking a maneuvering target's position and velocity. There exist other practical methods for tracking targets such as Kalman filtering [Park & Lee, 2001]. However, when the target motion is nonlinear and/or clutter and/or noise are non-Gaussian, this approach fails to be effective. Instead, unscented Kalman filter (UKF) and extended Kalman filter (EKF) come into use [Jian et al., 2007]. However, in long tailed noise, Kalman filtering results are

unsatisfactory. To overcome these difficulties, particle filtering (PF) is utilized [Jian et al., 2007].

Although particle filtering performs better than Kalman filtering in noisy environment, but it also diverges in low SNRs and cannot be trustable in this range of SNR. In addition, this method requires much more processing. We note that Kalman filtering, extended Kalman, unscented Kalman and particle filtering are recursive in nature. The new procedure proposed in this chapter is not recursive and can be used in the non-Gaussian, non-stationary noise, and nonlinear target motion. In here, the target tracking is performed based on the estimated time delay and Doppler. Since the accuracy of the time delay and Doppler estimation are high enough even in the severe noise, the results in tracking are acceptable compared to other rival approaches.

In section II the moment concept is reviewed and moment method is described as the base item in our estimations. Section III provides a model for the received signal. This signal has been influenced by unknown noise, delay and Doppler. It is shown in Section IV that it is possible to estimate Doppler by using the moments of the received random signal. The method is also useful for delay estimation. The noise power and its behavior play a prominent role in our work. So some analysis in this field is presented in this section too. After the parameter estimation, section V is devoted to explain about how the tracking a target is done based on the estimated delay and Doppler. And finally, section VI contains results that illustrate the effectiveness of the proposed method.

2. Moment concept

In probability theory, the moment method is a way in which the moments of a discrete sequence are used to determine its distribution.

Suppose that X is a random variable, and $f_X(x)$ is the probability density function (PDF) of this random variable. The moments of the random variable X is calculated from the following equation:

$$m_n = E\left(X^n\right) = \int_{-\infty}^{\infty} x^n f_X\left(x\right) dx = \int_{-\infty}^{\infty} x^n \, dF_X\left(x\right) dx, \tag{1}$$

which $F_X\left(x\right)$ is the cumulative distribution function (CDF) of the random variable X, and $E(.)$ is the expectation value.

On the other hand, the moment generating function (MGF) of this random variable is calculated as follows:

$$M_X\left(u\right) = E\left(e^{uX}\right), \quad u \in \mathbb{C}. \tag{2}$$

Note that the equation will be hold if the expectation value exists.

In here, to obtain the moments of a random variable, the relation between the moment and the moment generating function is use instead of using equation (1). This relation can be demonstrated as follows:

$$M_X\left(u\right) = E\left(e^{uX}\right) = \int_{-\infty}^{\infty} e^{ux} f_X\left(x\right) dx =$$

$$\int_{-\infty}^{\infty} (1 + ux + \frac{u^2x^2}{2!} + \cdots) f_X(x) dx = 1 + um_1 + \frac{u^2 m_2}{2!} + \cdots . \tag{3}$$

This equation is hold when the moments m_n are finite, i.e. $|m_n| < \infty$.

The moment method claims that using the moment of the random variable X, the PDF of X is completely determined. So if we have:

$$\lim_{n\to\infty} E\left(X_n^k\right) = E\left(X^k\right), \qquad \forall k \tag{4}$$

then, the sequence $\{X_n\}$ has the same distribution as the X. we use (4) for parameter estimation, i.e. The left side of the equation is obtained statically, and the right side is calculated analytically. These two sides should be equal.

To begin our discussion, a model should be considered for our signals. Next section is focused on finding the suitable model.

3. Signal model

We consider the baseband representation of the received signal, which can be expressed as the sum of the desired signal component and non-stationary background noise. The signal component is represented by the linear sum of many non-coherent waveforms whose arrivals at the receiver are governed by a Poisson process [Zabin & Wright, 1994]. The receiver includes two sensors to measure the received signal in presence of background noise:

$$\begin{aligned} y_1(t) &= s(t) + \omega_1(t), \\ y_2(t) &= s(t-\tau)\exp(j2\pi t\varepsilon) + \omega_2(t), \end{aligned} \tag{5}$$

where τ and ε denote the time delay and Doppler respectively, and $s(t)$ is the desired received signal modeled at any time instance t to follow a real N-mode Gaussian mixture distribution [Isaksson et al., 2001]:

$$s(t) \sim \sum_{i=1}^{N} p_i\, N\left(\mu_{s_i}, \sigma_{s_i}^2\right). \tag{6}$$

The processes $\omega_1(t)$ and $\omega_2(t)$ are real zero-mean additive white Gaussian noises (AWGN) with powers of $\sigma_{\omega_1}^2$ and $\sigma_{\omega_2}^2$ respectively. These powers are not constant in practice due to nonhomogeneous environment, but are assumed as random variates which are estimated subsequently. The signal and noise are supposed to be uncorrelated, but the noises $\omega_1(t)$ and $\omega_2(t)$ are possibly correlated.

4. Parameter estimation

In this section, for a random variable X, the moment generating function (MGF), $M_x(u)$, and its asymptotic series are used to determine the moments m_{xi}:

$$M_x(u) = E(e^{uX}) = 1 + um_{x1} + \frac{u^2 m_{x2}}{2!} + \cdots, \quad u \to 0. \tag{7}$$

4.1 Time delay estimation

The statistical properties of the signal and noise which are represented in (5) are known. Therefore, their MGF is available, by assuming finite moments of signal and noise. Although the signal follows a Gaussian mixture distribution, the conglomerate effect of the time delay

n	Moment	Central moment	Cumulant
0	1	1	–
1	μ	0	μ
2	$\mu^2+\sigma^2$	σ^2	σ^2
3	$\mu^3+3\mu\sigma^2$	0	0
4	$\mu^4+6\mu^2\sigma^2+3\sigma^4$	$3\sigma^4$	0

Table 1. Normal distribution moments

and Doppler creates a non-stationary signal, as seen in (5). At first, by using both sensors in the receiver, the time delay is predicted, then this estimated delay facilitates determination of the Doppler shift subsequently. The time delay estimation is described here and discussions about the Doppler estimation are provided in the sequel. It is required to consider the MGF of the normal distributed variate as the starting ground for the next steps:

$$M(u)=\exp\left(\mu u+0.5\sigma^2u^2\right), \tag{8}$$

where μ and σ are the mean and variance of normal distribution. The related moments are depicted in table (I). We suppose the received noise-free signal in the second sensor is denoted by:

$$r(t)=s(t-\tau)\exp(j2\pi t\varepsilon). \tag{9}$$

First, we assume there is no Doppler i.e. $r(t)=s(t-\tau)$, and the noise variances, $\sigma^2_{\omega_1}$ and $\sigma^2_{\omega_2}$, are constant. As mentioned above, we utilize the MGF for the estimation purposes. The noise terms in both sensors have normal distributions. Since the noise terms in (5) and signal $s(t)$ are independent, the difference between MGF of two received signals $y_1(t)$ and $y_2(t)$ in (5) is derived from the noise-free terms $s(t)$ and $r(t)$. Since $r(t)$ is the delayed replica of $s(t)$, it includes two blocks. When the second sensor has not sensed the received signal yet, $r(t)$ merely contains the noise $\omega_2(t)$ and its MGF can be calculated by (8), but, as soon as the transmitted signal arrives at this sensor, $y_2(t)$ shows a similar behavior to $y_1(t)$. This suitable observation could be used for the time delay estimation.

So, MGF of signal detected at the first sensor is considered as a reference for our estimation in the second sensor. Indeed, the moments of $y_1(t)$ are extractable from this known MGF by using (7). These moments are employed as the reference for comparing among results retrieved from the second sensor. In the second sensor, a rectangular running window is implemented on $y_2(t)$ and this window helps to extract different segments of $y_2(t)$ step by step. The window length depends on two parameters. First, it must be long enough to be trustable in calculating the estimated moments, on the other hand, it should not be so long that damages the real-time characteristics of estimator. Anyway, there is a trade-off between these two factors. The window length is considered constant and moves from the beginning

of the signal to the end. Besides the length, the overlap between adjacent frames is another item that is determined according to the required accuracy and tolerable complexity in the time delay estimation. At the beginning of signal block, the windowed signal includes only the noise part of $y_2(t)$, because of delay τ, so it exhibits different moments in comparison with $y_1(t)$. While the first point of window reaches the onset of delayed signal $s(t-\tau)$, the estimated moments become similar to the moments of $y_1(t)$. Mean square error (MSE) criterion is applied for observing the measure of this similarity. At first, we observe large MSE values, but, the window progression leads to a decrease in MSE and after the τ seconds delay point, we get a small amount for MSE nearly equal to zero and will remain constant up to the end of observation time.

Now, Doppler is considered and $r(t)$ is obtained from (9). Doppler changes the constant amount of MSE which had happened after τ seconds. It means that after the delay point, Doppler increases MSE *g*radually, but this phenomenon is not an annoying event in time delay estimation, even it helps to find the time delay, because this increasing in MSE takes place from the delay point, so it causes the delay point to be the point which has minimum value for MSE.

In figure (1), the Doppler effect on the MSE behavior is showed for three different SNRs. Time delay is equal to 300 microseconds. In SNR=+10dB, the result is clear. In two other SNRs, the minimum point is almost matched well with the actual amount of delay, i.e. 300.

We assume the windowed signal in the *k*-th step of window moving is denoted by y_{2k} and the *i*-th moment of this windowed signal is presented as $\hat{m}_{y_{2k},i}$. Therefore, the *k*-th window whose related moments $\hat{m}_{y_{2k},i}$ are the most similar to those of $y_1(t)$, $m_{y_1,i}$, can be estimated by:

$$\hat{k} = \arg\min_{k} \sum_{i=1}^{L} \left| m_{y_1,i} - \hat{m}_{y_{2k},i} \right|^2, \tag{10}$$

where in here, L is considered 4, and it would reveal a desirable result [Fukunaga et al., 1983]. In fact, when L=4, we use 4 moments of signal. So we have 4 equations that are applied to determine the unknown parameter. Although there is only one unknown parameter, but the noise signal does not let us find the parameter by only one equation. But the use of four equations is enough. Note that if more accuracy is needed, L can be considered larger. So, the delay point, $\hat{\tau}$, is the first point of $\hat{k}$-th window.

Despite the presence of Doppler, the proposed moment method estimates the time delay precisely. Consequently, this method can consider the time delay and Doppler simultaneously, and thus, is able to estimate the joint time delay and Doppler accurately.

4.2 Doppler estimation

In this section, we can consider the estimated delay $\hat{\tau}$ as the time origin for the received signal in the second sensor:

$$y_2(t+\hat{\tau}) = r(t+\hat{\tau}) + \omega_2(t+\hat{\tau}), \quad t \geq 0. \tag{11}$$

According to (9) and (11), we have:

$$y_2(t+\hat{\tau}) = s(t)\exp(j2\pi(t+\hat{\tau})\varepsilon) + \omega_2(t+\hat{\tau}), \quad t \geq 0. \tag{12}$$

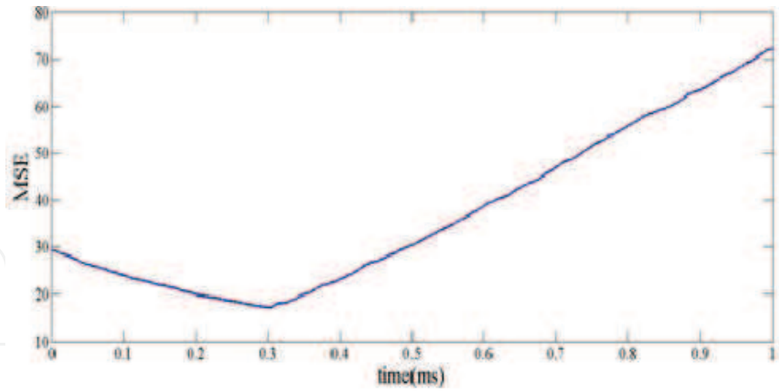

a) SNR=+10 dB

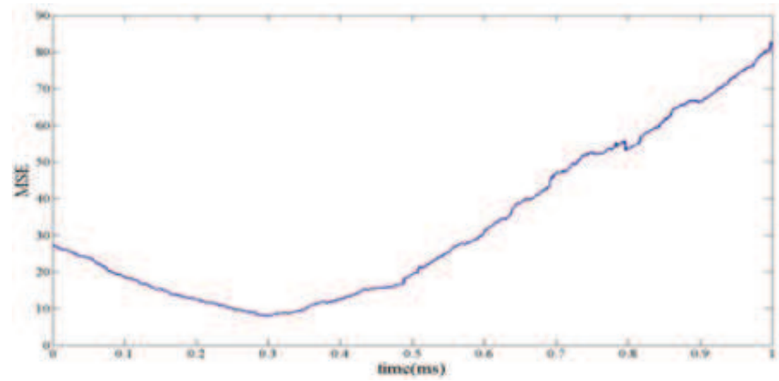

b) SNR= 0 dB

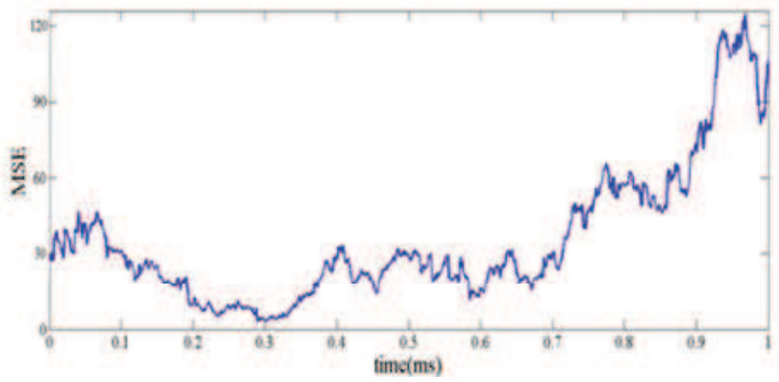

c) SNR=-10 dB

Fig. 1. MSE between the signal $y_1(t)$ moments and the windowed parts of signal $y_2(t)$ moments. a) SNR=+10dB, b) SNR=0dB, c) SNR=-10dB

Doppler and noise effect on the moments of $y_2(t+\hat{\tau})$ should be noticed. Instead of $y_2(t+\hat{\tau})$, we work on the real part:

$$y_{2r}(t+\hat{\tau}) = s(t)\cos(2\pi(t+\hat{\tau})\varepsilon) + \omega_2(t+\hat{\tau}), \quad t \geq 0. \tag{13}$$

$y_{2r}(t+\hat{\tau})$ includes the noise and signal, and the signal is also affected by Doppler which changes the moments of the signal. Therefore, we prefer to obtain MGF of $y_{2r}(t+\hat{\tau})$ firstly, then, the moments are obtained from this MGF by (7). The noise-free signal in (13) is independent from the noise $\omega_2(t+\hat{\tau})$, so MGF of $y_{2r}(t+\hat{\tau})$ is:

$$M_{y_{2r}}(u) = M_r(u)M_{\omega_2}(u), \tag{14}$$

where $M_r(u)$ is MGF of the first term in right side of (13), and:

$$M_{\omega_2}(u) = \exp\left(0.5\sigma_{\omega_2}^2 u^2\right). \tag{15}$$

The time varying variance will be comprehensively discussed in the sequel. Here, the problem is to estimate $M_r(u)$. $s(t)$ follows a Gaussian mixture distribution in (6). The presence of the cosine term changes the first term in the right side of (13) to a non-stationary process. Although the cosine term is time variant, fortunately, it is deterministic.

Now, we obtain $M_r(u)$:

$$\begin{aligned} M_s(u) &= \sum_{i=1}^{N} p_i \exp\left(\mu_{s_i}u + 0.5\sigma_{s_i}^2 u^2\right) \quad \Rightarrow \\ M_r(u;t) &= \sum_{i=1}^{N} p_i \exp\left(\mu_{s_i}u + 0.5\sigma_{s_i}^2 \cos^2(2\pi(t+\hat{\tau})\varepsilon)u^2\right). \end{aligned} \tag{16}$$

Both $M_r(u)$ and $M_{\omega_2}(u)$ are expressed as the series for $u \to 0$, then by multiplying these two series and ordering their terms, MGF of $y_{2r}(t+\hat{\tau})$ is asymptotically obtained in the context of (7):

$$\begin{aligned} M_{y_{2r}}(u) &= M_r(u)\, M_{\omega_2}(u) \\ &= (1 + um_{r1} + \frac{u^2 m_{r2}}{2!} + \frac{u^3 m_{r3}}{3!} + \frac{u^4 m_{r4}}{4!} + \cdots) \\ &\times (1 + um_{\omega_2 1} + \frac{u^2 m_{\omega_2 2}}{2!} + \frac{u^3 m_{\omega_2 3}}{3!} + \frac{u^4 m_{\omega_2 4}}{4!} + \cdots) \\ &= 1 + u(m_{r1} + m_{\omega_2 1}) + \frac{u^2(m_{r2} + m_{\omega_2 2} + 2m_{r1}m_{\omega_2 1})}{2!} \\ &+ \frac{u^3(m_{r3} + m_{\omega_2 3} + 3m_{r1}m_{\omega_2 2} + 3m_{r2}m_{\omega_2 1})}{3!} \\ &+ \frac{u^4(m_{r4} + m_{\omega_2 4} + 6m_{r2}m_{\omega_2 2} + 4m_{r1}m_{\omega_2 3} + 4m_{r3}m_{\omega_2 1})}{4!} + \cdots. \end{aligned} \tag{17}$$

The moments extracted from $M_r(u)$ are shown in Table (II). There exists also another problem. The resulting moments of $y_{2r}(t+\hat{\tau})$ are time dependent. Since the cosine term is deterministic, the time average of the moments can be substituted instead. Let's define:

$$\zeta_i(\varepsilon) = \frac{1}{T}\int_0^T \cos^i(2\pi(t+\hat{\tau})\varepsilon)dt, \tag{18}$$

n Moment
0 1
1 $\sum_{i=1}^{N} p_i \mu_{s_i}$
2 $\sum_{i=1}^{N} p_i (\mu_{s_i}^2 + \sigma_{s_i}^2 \cos^2(2\pi(t+\hat{\tau})\varepsilon))$
3 $\sum_{i=1}^{N} p_i (\mu_{s_i}^3 + 3\mu_{s_i}\sigma_{s_i}^2 \cos^2(2\pi(t+\hat{\tau})\varepsilon))$
4 $\sum_{i=1}^{N} p_i (\mu_{s_i}^4 + 6\mu_{s_i}^2\sigma_{s_i}^2 \cos^2(2\pi(t+\hat{\tau})\varepsilon) + 3\sigma_{s_i}^4 \cos^4(2\pi(t+\hat{\tau})\varepsilon))$

Table 2. Moments extracted from $M_r(u;t)$

where T is the observation time. Note that for dependency of $\zeta_i(\varepsilon)$ on ε, the moments of $y_{2r}(t+\hat{\tau})$ are dependent on ε too. Finally, for obtaining the time-independent moments of $y_{2r}(t+\hat{\tau})$, $m_{y_{2r},i}$, it suffices that all "$\cos^i(2\pi(t+\hat{\tau})\varepsilon)$" terms in the time-dependent moments to be substituted by $\zeta_i(\varepsilon)$. The final moments are depicted in table (III).

Since now, the moments were obtained analytically, it means we only calculated the right side of equation (4). On the other hand, the moments of the observed signal in the second receiver can be calculated statistically by:

$$\tilde{m}_i = \frac{1}{T}\int_0^T y_{2r}^i(t+\hat{\tau})dt. \tag{19}$$

Now the left side of the equation (4) is also obtained. Both of these two procedures must yield same results. Thus, ε should be selected in such a way that this equality holds. To do this, MSE criterion is used again:

$$\text{MSE} = \sum_{i=1}^{L} \left| m_{y_{2r},i} - \tilde{m}_i \right|^2. \tag{20}$$

Similar to the previous section, L is considered as 4. So Doppler of the received signal $y_{2r}(t+\hat{\tau})$ is estimated:

$$\hat{\varepsilon} = \arg\min_{\varepsilon} \sum_{i=1}^{L} \left| m_{y_{2r},i} - \tilde{m}_i \right|^2. \tag{21}$$

4.3 Noise power estimation

The noise power estimation is similar to Doppler estimation. Indeed, these two estimations are done simultaneously. It could be seen that the moments do not merely depend on Doppler.

n Moment	
0	1
1	$\sum_{i=1}^{N} p_i \mu_{s_i}$
2	$\sum_{i=1}^{N} p_i(\mu_{s_i}^2 + \sigma_{s_i}^2 \zeta_2(\varepsilon)) + \sigma_\omega^2$
3	$\sum_{i=1}^{N} p_i \left(\mu_{s_i}^3 + 3\mu_{s_i}\sigma_{s_i}^2 \zeta_2(\varepsilon)\right) + 3\sigma_\omega^2 \sum_{i=1}^{N} p_i \mu_{s_i}$
4	$\sum_{i=1}^{N} p_i \left(\mu_{s_i}^4 + 6\mu_{s_i}^2 \sigma_{s_i}^2 \zeta_2(\varepsilon) + 3\sigma_{s_i}^4 \zeta_4(\varepsilon)\right) + 3\sigma_\omega^4 + 6\sigma_\omega^2 \sum_{i=1}^{N} p_i(\mu_{s_i}^2 + \sigma_{s_i}^2 \zeta_2(\varepsilon))$

Table 3. Final moments extracted from $M_{y_{2r}}(t+\hat{\tau})$

They depend onto the noise power as well. So, in (20), MSE includes two parameters, the noise power and Doppler of the received signal, and should be minimized according to both of them:

$$(\hat{\varepsilon}, \hat{\sigma}_{\omega_2}^2) = \arg\min_{\varepsilon, \sigma_{\omega_2}^2} \sum_{i=1}^{L} \left| m_{y_{2r},i} - \tilde{m}_i \right|^2. \tag{22}$$

Now it is the time to discuss about the variable variance of the noise. This means that in (14) the noise variance is considered unknown. We can estimate the noise variance given N_1 signal-free samples which are at hand occasionally. So, $\sigma_{\omega_2}^2$ becomes a random variate. Since the noise $\omega_2(t+\hat{\tau})$ is assumed Gaussian, the N_1-sample based estimated variance is chi-square distributed with N_1 degrees of freedom:

$$\hat{\sigma}_{\omega_2}^2 = \frac{1}{N_1} \sum_{i=1}^{N_1} \omega_{2_i}^2, \quad \hat{\sigma}_{\omega_2}^2 \sim \chi_{N_1}^2. \tag{23}$$

Hence, the average MGF of the noise over σ^2 is obtained in (14) as:

$$\begin{aligned} \bar{M}_{\omega_2}(u) &= \frac{1}{\sqrt{(1 - \hat{\sigma}_{\omega_2}^2 u^2 / N_1)^{N_1}}} \\ &= 1 + 0.5\hat{\sigma}_{\omega_2}^2 u^2 + (0.125 + 1/4N_1)\hat{\sigma}_{\omega_2}^4 u^4 + \cdots. \end{aligned} \tag{24}$$

In this non-stationary noise scenario due to $\hat{\sigma}_{\omega_2}^2$, the procedure presented for Doppler estimation in the previous part does not change, only MGF and the moments of the normal

distribution considered previously for the noise should be substituted by the ones determined in (24).

5. Radar tracking

In the basic section, we said that the proposed parameter estimation can be useful for the tracking of a target. As mentioned, there are various methods for the target tracking which present specific mathematical algorithms. These methods have different performance levels, but most of them are recursive, so that at any time, the data is obtained by using previous data and improving them. Now, some of the most common procedures and their problems are expressed and then, the proposed moment method are described in detail.

5.1 Kalman filter

The Kalman filter is the central algorithm to the majority of all modern radar tracking systems. The role of the filter is to take the current known state (i.e. position, heading, speed and possibly acceleration) of the target and predict the new state of the target at the time of the most recent radar measurement. In making this prediction, it also updates its estimate of its own uncertainty (i.e. errors) in this prediction. It then forms a weighted average of this prediction of state and the latest measurement of state, taking account of the known measurement errors of the radar and its own uncertainty in the target motion models. Finally, it updates its estimate of its uncertainty of the state estimate. A key assumption in the mathematics of the Kalman filter is that measurement equations (i.e. the relationship between the radar measurements and the target state) and the state equations (i.e. the equations for predicting a future state based on the current state) are linear, i.e. can be expressed in the form $y = A.x$ (where A is a constant), rather than $y = f(x)$. The Kalman filter assumes that the measurement errors of the radar, and the errors in its target motion model, and the errors in its state estimate are all zero-mean Gaussian distributed. This means that all of these sources of errors can be represented by a covariance matrix. The mathematics of the Kalman filter is therefore concerned with propagating these covariance matrices and using them to form the weighted sum of prediction and measurement [Ristic et al., 2004].

In situations where the target motion conforms well to the underlying model, there is a tendency of the Kalman filter to become "over confident" of its own predictions and to start to ignore the radar measurements. If the target then manoeuvres, the filter will fail to follow the manoeuvre. It is therefore common practice when implementing the filter to arbitrarily increase the magnitude of the state estimate covariance matrix slightly at each update to prevent this.

5.2 Extended Kalman Filter (EKF)

This method is a class of nonlinear tracking algorithms that provides much better results than the Kalman filter.

Nonlinear tracking algorithms use a nonlinear filter to cope with the following cases:

- The relationship between the radar measurements and the track coordinates is nonlinear.
- The errors are nonlinear.
- The motion model, is non-linear.

In this case, the relationship between the measurements and the state is of the form $h = f(x)$ (where h is the vector of measurements, x is the target state and $f(.)$ is the function relating the two). Similarly, the relationship between the future state and the current state is of the form $x(t+1) = g(x(t))$ (where $x(t)$ is the state at time t and $g(.)$ is the function that predicts the future state). To handle these non-linearities, the EKF linearizes the two non-linear equations using the first term of the Taylor series and then treats the problem as the standard linear Kalman filter problem. Although conceptually simple, the filter can easily diverge (i.e. gradually perform more and more badly) if the state estimate about which the equations are linearized is poor. The unscented Kalman filter and particle filters are attempts to overcome the problem of linearizing the equations.

5.3 Particle Filtering (PF)

Another example of nonlinear methods is particle filtering. This method makes no assumptions about the distributions of the errors in the filter and neither does it require the equations to be linear. Instead it generates a large number of random potential states ("particles") and then propagates this "cloud of particles" through the equations, resulting in a different distribution of particles at the output. The resulting distribution of particles can then be used to calculate a mean or variance, or whatever other statistical measure is required. The resulting statistics are used to generate the random sample of particles for the next iteration. However, this method also has some problems that restrict the use. This method requires large computational operations and face severe difficulties for real-time applications. On the other hand, this method is also not able to have suitable results in very low SNRs. In these SNRs, PF is not able to bring us to a reasonable particle, and even using Sampling Importance Re-sampling (SIR) method can not lead us to better results [Ristic et al., 2004]. In SIR method, a weighted set of particles is used. These new weighted particles can face and eliminate the noise more powerfully and present better estimation in low SNRs.

5.4 The proposed moment method

In this section, we are going to solve the problems we are faced in PF. This is done based on the time delay and Doppler estimated in the previous section. Three sensors are used. They are located on the vertices of an equilateral triangle. One of the sensors is a transmitter and receiver, the other two sensors only serve as the receiver. The arrangement of the sensors and their positions relative to the target is depicted in figure (2). The target is in the far field of the sensors.

A signal is emitted from the first sensor to the target. When this signal comes into contact with the target, generally speaking, it is scattered in many directions. The signal is thus partly reflected back, hence, all three sensors receive this reflected signal. According to the earlier discussions, the time delay and Doppler of the received signal in each sensor could be estimated.

First, the target position is determined. Suppose the time interval between sending the signal from the transmitter and receiving it in each sensor is shown by $T_i \ for \ \ i = 1, 2, 3$, which i denotes the sensor number. We also use R_i as the distance between the target and the i-th receiver. Since the transmitter is beside the first receiver, we have:

$$R_1 = \frac{1}{2} T_1 \times C_e, \tag{25}$$

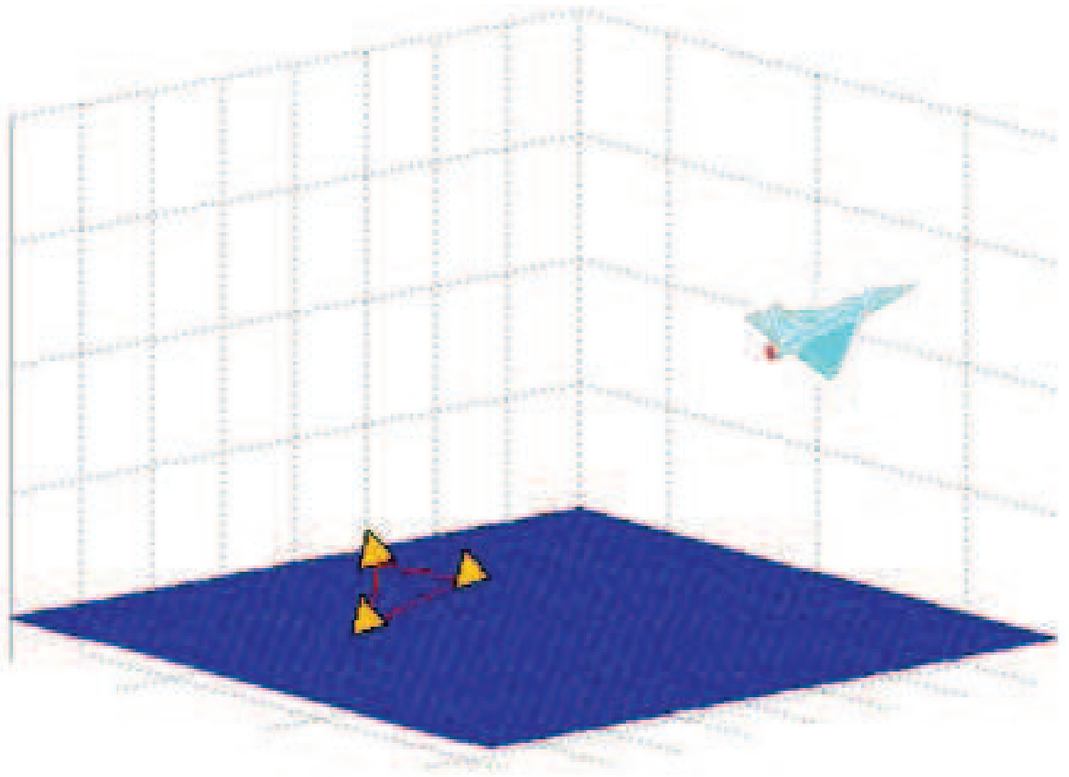

Fig. 2. The arrangement of the three sensors and their positions relative to the target

which C_e is the velocity of the emitted signal that is equal to the light speed. For two other receivers that are not near the transmitter, the distance is calculated as:

$$R_i = (T_i - \frac{T_1}{2}) \times C_e, \quad i = 2, 3. \tag{26}$$

Each sensor provides the locus of the target on a sphere of radius R_i centered at that sensor. As mentioned before, these sensors are located on the vertices of an equilateral triangle.

It can be shown mathematically that the intersection of these three spheres is at two points. To prove this, the equations for the three spheres are considered, and then the intersection of them is obtained. Without losing the generality, we assume that the three points where the sensors are located in, are showed by A, B and C. The points are respectively in $(x_0, 0, 0)$, $(-x_0, 0, 0)$ and $(0, y_0, 0)$ in Cartesian coordinates and are showed in figure (3).

At first, the equations of two spheres with centers A and B and radii R_1 and R_2 are obtained:

$$\begin{aligned} (x - x_0)^2 + y^2 + z^2 &= R_1^2, \\ (x + x_0)^2 + y^2 + z^2 &= R_2^2. \end{aligned} \tag{27}$$

The first equation is subtracted from the second one:

$$\begin{aligned} 2xx_0 - (-2xx_0) &= R_2^2 - R_1^2 \quad \Rightarrow \\ 4xx_0 = R_2^2 - R_1^2 \quad &\Rightarrow \quad x = \frac{R_2^2 - R_1^2}{4x_0}. \end{aligned} \tag{28}$$

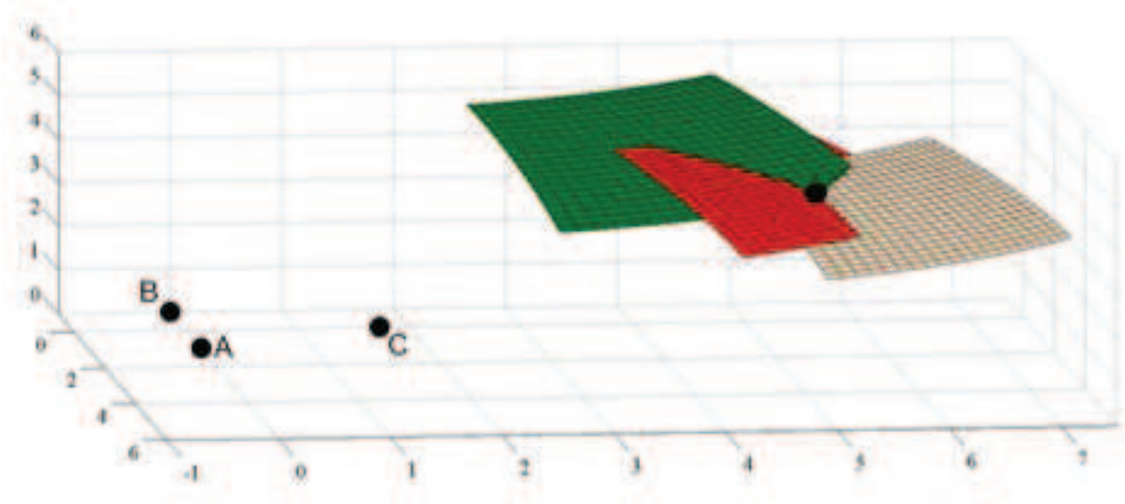

Fig. 3. The position of the three sensors and the intersection of three spheres related to the sensors

Now, the obtained value x is put in the one of the equations (27). We select the first one:

$$\left(\frac{R_2^2 - R_1^2}{4x_0} - x_0\right)^2 + y^2 + z^2 = R_1^2 \quad \Rightarrow$$
$$y^2 + z^2 = R_1^2 - \left(\frac{R_2^2 - R_1^2}{4x_0} - x_0\right)^2. \tag{29}$$

For convenience, the right side of the second equality of (29) is showed by R_{cir}^2. Thus, the intersection of the two spheres is a circle with the following equation:

$$y^2 + z^2 = R_{cir}^2, \tag{30}$$

Which is located in the plane $x = \frac{R_2^2 - R_1^2}{4x_0}$.

Then the intersection of this circle and the third sphere should be obtained. The third sphere has the center C and radius R_3. So its equation is:

$$x^2 + (y - y_0)^2 + z^2 = R_3^2. \tag{31}$$

The left side of the equation (31) is extended, and the circle equation is used in it:

$$\begin{aligned} x^2 + (y - y_0)^2 + z^2 &= -2yy_0 + y_0^2 + x^2 + y^2 + z^2 \\ &= -2yy_0 + y_0^2 + \left(\frac{R_2^2 - R_1^2}{4x_0}\right)^2 + R_{cir}^2 \quad \Rightarrow \\ y &= \frac{y_0^2 + \left(\frac{R_2^2 - R_1^2}{4x_0}\right)^2 + R_{cir}^2}{2y_0}. \end{aligned} \tag{32}$$

So, x and y coordinates of the intersection point is:

$$x = \frac{R_2^2 - R_1^2}{4x_0}$$
$$y = \frac{y_0^2 + \left(\frac{R_2^2 - R_1^2}{4x_0}\right)^2 + R_{cir}^2}{2y_0}. \tag{33}$$

Using this two values and the equation (31), the third coordinates is also calculated:

$$z = \pm \sqrt{R_3^2 - \left(\frac{R_2^2 - R_1^2}{4x_0}\right)^2 - \left(\frac{y_0^2 + \left(\frac{R_2^2 - R_1^2}{4x_0}\right)^2 + R_{cir}^2}{2y_0} - y_0\right)^2}. \tag{34}$$

As mentioned, this intersection contains only two points which are located in the two sides of the plane xy and in front of each other. But in reality, only one of these points has a positive height and coincides with the coordinate of a target in sky.

After this proof, we continue our discussion about the tracking. On the one hand, the target position is achievable by using R_is, and on the other hand, the equations (25) and (26) inform about the relation between R_is and T_is. Therefore, the target position can be determined if T_i is known. For calculating this parameter, it should be considered as the signal's time delay to reach to the i-th receiver. Let's assume the first sensor in the section (IV), is the transmitter now, and the second sensor in there is one of the three receivers in here. By using the proposed moment method three times, the time delay can be estimated for all the three receivers. T_i is denoted as the estimated time delay for i-th receiver. Now, all unknowns are obtained, so the position is easily predicted.

Finally, the target velocity should be obtained. The receivers compute three values for Doppler, $\hat{\varepsilon}_i$, by the proposed moment technique. Since the transmitter and the first receiver are at the same sensor, the velocity component along the connecting line between the target and the first sensor is:

$$v_1 = \frac{d}{dt}\|\boldsymbol{R_1}\| = \frac{C}{2f_t}\,\hat{\varepsilon}_1, \tag{35}$$

where $\|.\|$ represents Euclidean norm, and $\boldsymbol{R_1}$ is the vector connecting the first sensor to the target. C is the speed of light and f_t is the frequency of the emitted signal. Using v_1, we determine the velocity components along the connecting line between the target and two other sensors (receivers):

$$v_i = \frac{C}{f_t}\,\hat{\varepsilon}_i - v_1, \quad i = 2, 3. \tag{36}$$

In the next section, there are results that compare the different methods available for estimating the time delay and Doppler. There are also some results about tracking a target which has a nonlinear motion. In the parameter estimation results, the proposed moment method is compared with the methods Wigner-Ville (WV), fractional lower order ambiguity function (FLOAF) and wavelet, and in the tracking part, there is a comparison between the proposed method and EKF and PF ones.

6. The results

To prove the procedures were presented in this Chapter, several different tests have been conducted. The results are divided into two categories. At first, the proposed method for estimating the joint time delay and Doppler is examined and compared with other conventional methods. Then, the efficiency of this method in the tracking of the maneuver target is also investigated.

6.1 Parameter estimation results

To estimate the time delay and Doppler parameters, the following assumptions are considered:

- The transmitted desired signal follows a trimodal Gaussian mixture distribution presented in equation (6) with the following mean and standard deviation related to the three modes:
  $\sigma_{s_1} = \sigma_{s_2} = \sigma_{s_3} = 1$,
  $\mu_{s_1} = 2$, $\mu_{s_2} = 5$, $\mu_{s_3} = 8$,

  And the probability distribution of the modes is considered as below:
  $p_1 = 0.3,\ p_2 = 0.3,\ p_3 = 0.4$.

- The observation time of the signal is considered 1 millisecond.

- The time delay can be within the observation time of the signal, and in here, it is assumed 300 microseconds.

- Doppler value, $\omega_\varepsilon = 2\pi\varepsilon$, is a number between 0 and 2π that provides a 2π rotation for the frequency shift. Now, Doppler is assumed 0.8π.

The test is done for different SNR values from -10dB to +10dB, and for each SNR, the operation is performed 1000 times. The figure (4) depicts the error existed in the estimation of the time delay for the conventional methods and the proposed moment one. This error is depicted as MSE, calculated from 1000 times of simulation implementation, versus SNR. We have used normalized MSE in our results:

$$MSE\left(\hat{\tau}\right) = E\left[\left(\frac{\hat{\tau}-\tau}{\tau}\right)^2\right], \tag{37}$$

where τ is the actual time delay, and $\hat{\tau}$ is the estimated value of this parameter. The conventional methods are WV [Chassande-Mottin & Pai, 2005], wavelet method [Niu et al., 1999] and FLOAF [Ma & Nikias, 1996].

As shown in Figure (4), all methods are convincing in high SNRs, but in low SNRs, especially negative ones, WV and FLOAF methods are completely unable to estimate the time delay. Wavelet method also has relatively unsuitable results, so that it presents very little reduction in MSE value from SNR=-10dB to SNR=0dB. But the moment method in the both high and low SNRs provides precise answers.

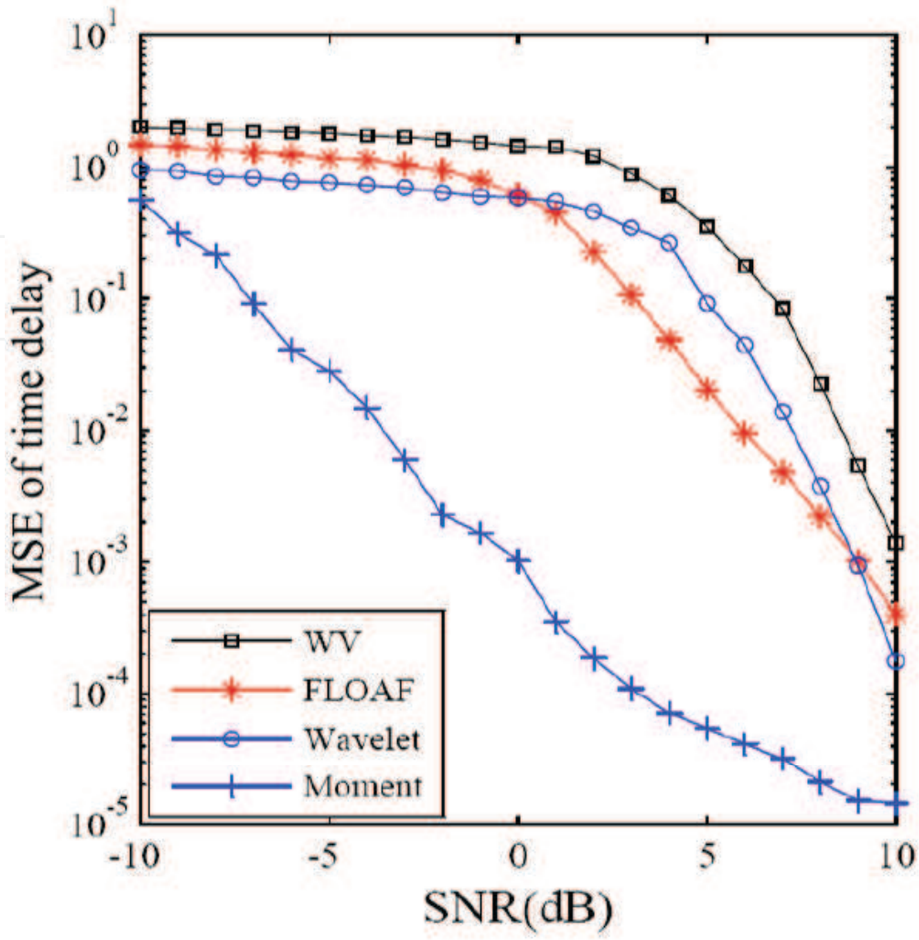

Fig. 4. MSE of estimated time delay in the conventional and proposed methods.

There is a similar observation for Doppler that is showed in figure (5). The error is also as MSE versus SNR. In this figure, the conventional methods are WV [Chassande-Mottin & Pai, 2005] and FLOAF [Ma & Nikias, 1996].

As portrayed in figure (5), WV offers very good results in high SNRs which is expectable. But in the low SNRs, the interaction terms are relatively large and this method fails. So in low SNRs, FLOAF presents more suitable results in comparison with WV. Again in this figure, the power of moment method is absolutely visible.

It is worth mentioning that the obtained results are in an unknown noise power scenario. The moment method also can estimate the noise power. It is important that in addition to parameter estimation, our method can also predict the noise power. This capability helps to recognize the noise environment, and ameliorates noise encountering. To judge the performance of the proposed moment method for estimating the unknown noise power, MSE between the actual and the estimated noise power is portrayed in figure (6). For instance, MSE is 10^{-5} in SNR 8. It means that in this SNR, we have an error between the actual noise power

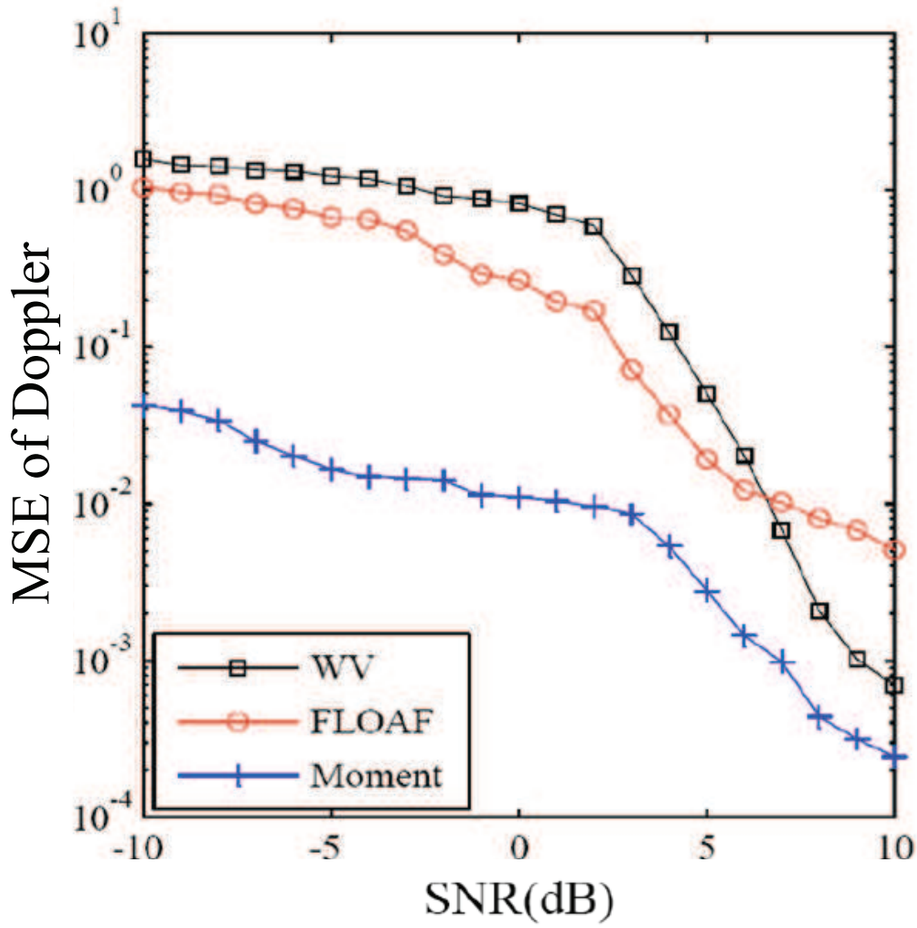

Fig. 5. MSE of estimated Doppler in the conventional and proposed methods.

and the value which our method has estimated for it, and the normalized mean square value of this error is equal to 10^{-5}.

6.2 Radar tracking results

In the following, radar tracking results are presented based on the time delay and Doppler estimations. The original frequency of the signal emitted from the radar, f_t, is considered $10GHz$. A target is at cartesian coordinate $(10000m, 10000m, 10000m)$. It moves with the velocity $v_x = 10m/s, v_y = 10m/s$. In the first 25 sec, $v_z = -10$ m/s and in the following 75 sec, v_z=+20 m/s. At first, for SNR=+10dB, test is done for the non-recursive proposed moment method and two recursive conventional methods: EKF [Park & Lee, 2001] and PF [Jian et al., 2007]. The results have been traced for 100 epochs with one second interval and can be seen in figures (7) and (8) as MSE of the estimated position and velocity.

Two points are worth noting in this figures. EKF and PF methods are recursive, so the related curves are decreasing and at first, have not acceptable results. We need some time to have suitable results. In vital application like military, less needed time leads us to a better real-time system and gives the opportunity to react faster. So, a non-recursive method can be valuable.

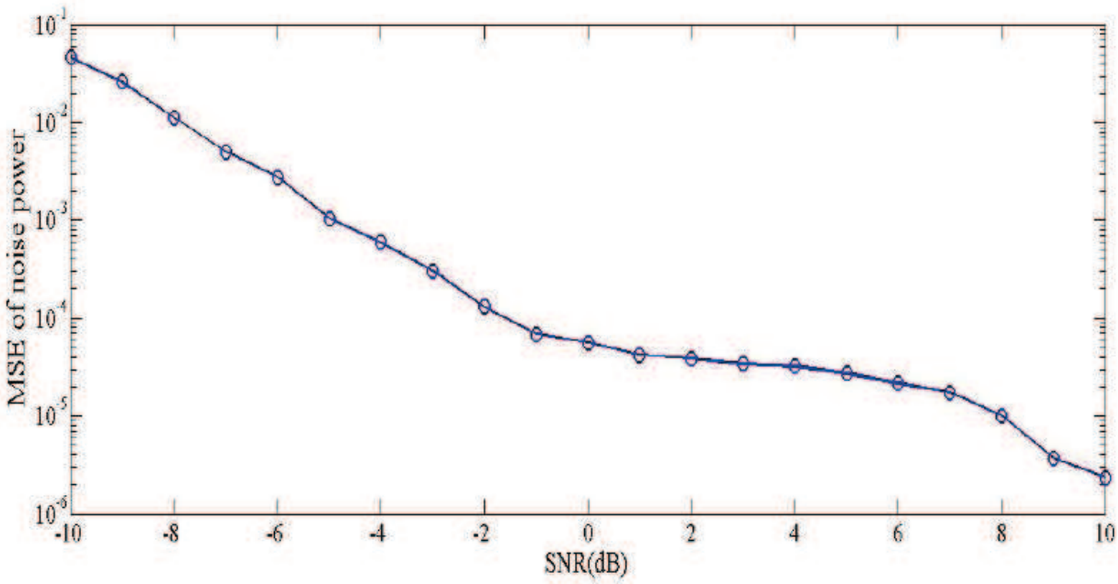

Fig. 6. MSE of estimated noise power in the proposed method

In addition to have a high precision, the moment method is non-recursive, trustable from the beginning, and provides a rapid reaction.

The second point in figures (7) and (8) is the existence of a bulge around the time 25 seconds, where the third component of the speed has changed and made a nonlinear motion. There is no bulge in the curves relating to the moment method, because in this method, the estimation at any time is independent from the other times, so it has no problem in nonlinear motions. In the figures we magnify the results around time 25 seconds and show them in linear scale to depict the bulge obviously. We cannot present all results together in linear scale, because moment results are too small in comparison with EKF and PF results.

To further examine the ability of the proposed method, the test is done at different SNRs. The results of this experiment is showed in figures (9) and (10). In the figures, MSE of the position and velocity estimation is portrayed for our moment method.

In figures (7) and (8), MSE is versus time , and SNR is constant and equal to +10dB. Thus the figures (7) and (8) show the superiority of the proposed method on the two other ones. But in figures (9) and (10), MSE is versus SNR. The power of moment method in the low SNR is quite satisfactory, while the other methods, the EKF and PF, either do not respond or provide answers that are not reliable.

Finally, a necessary point should be noted. We see that our method has much better results in comparison with other ones. The better results are not only because of using moments. Moment method helps us as a tool to encounter the undesired signals logically. In fact, in the first step, we recognize the environment more precisely by a suitable model of noise. Then after the modelling, although the noise is unknown, but the moments of its model are known and used for our estimations. So we can control the noise behaviour. This procedure cannot be found in other methods.

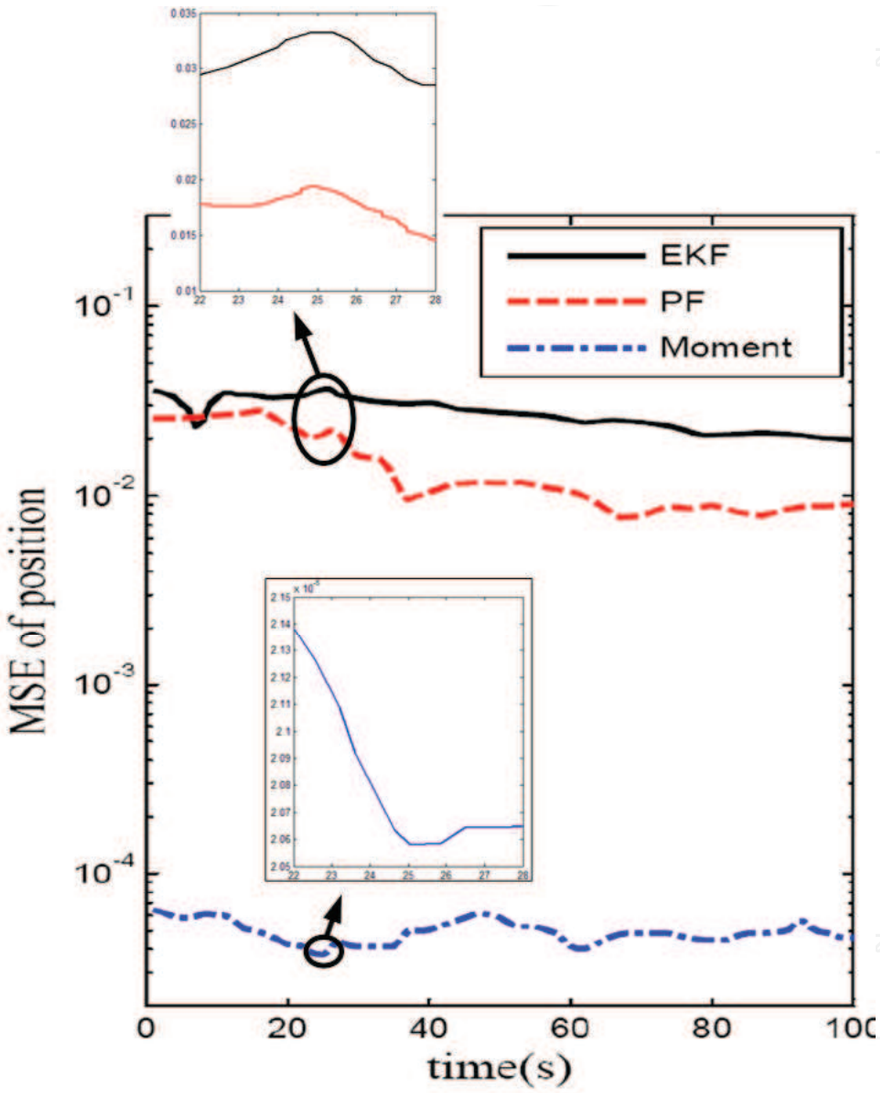

Fig. 7. MSE of estimated position in the conventional and proposed methods for SNR=+10 dB.

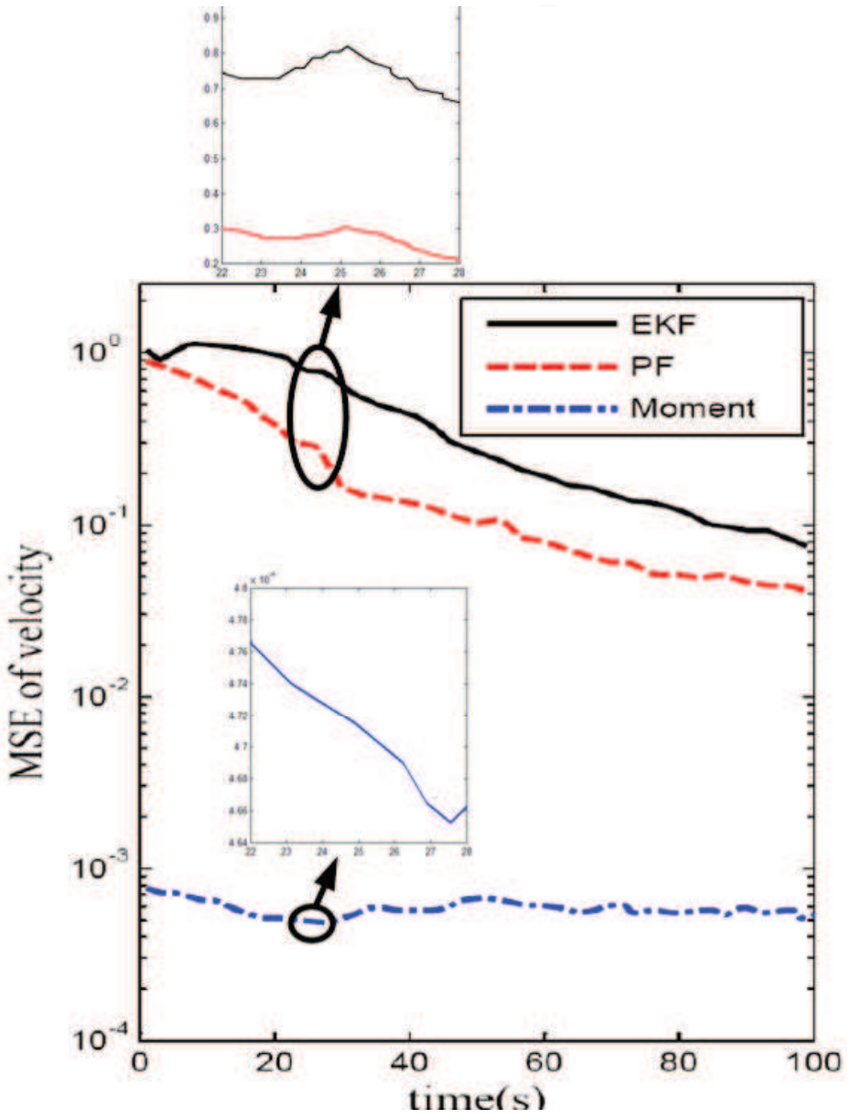

Fig. 8. MSE of estimated velocity in the conventional and proposed methods for SNR=+10 dB.

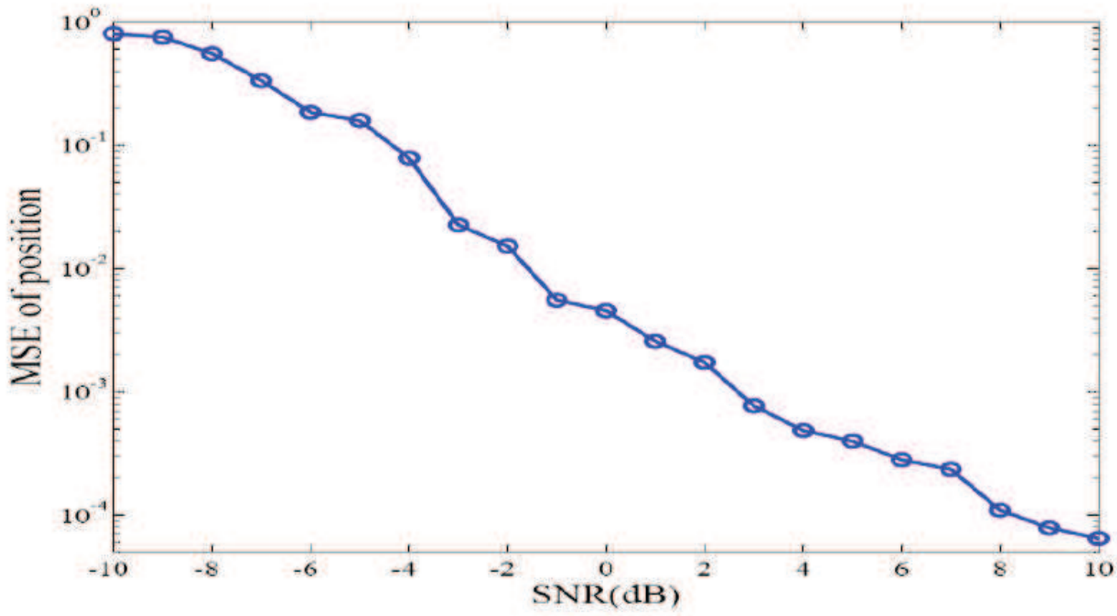

Fig. 9. MSE of estimated position in the proposed method.

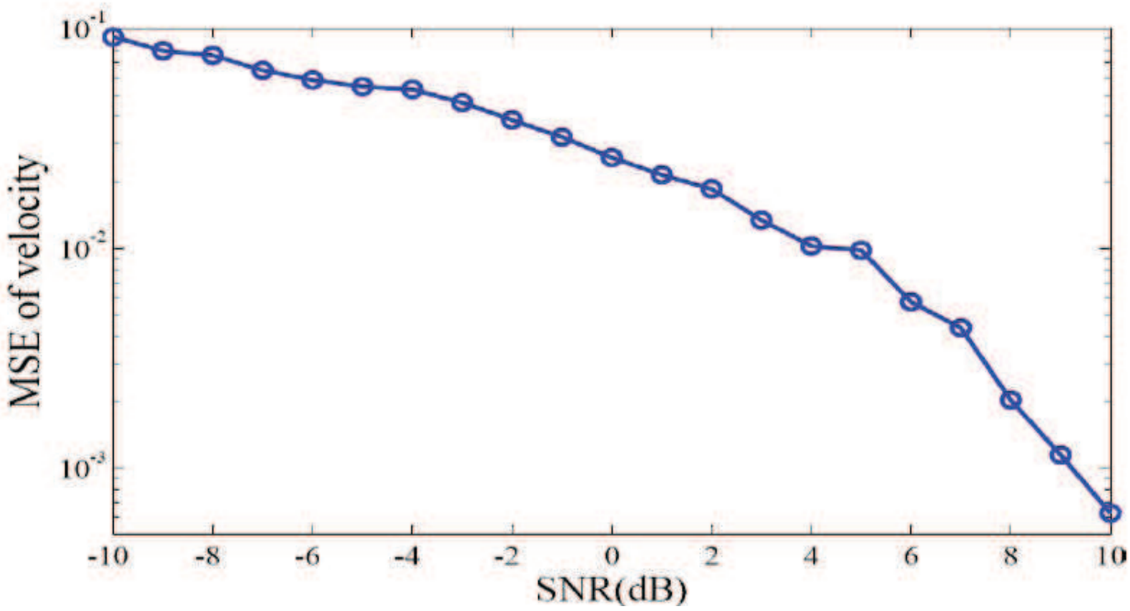

Fig. 10. MSE of estimated velocity in the proposed method.

7. Conclusion

In this chapter, we review different novel methods in joint time delay and Doppler estimation. Each of them has some advantages and disadvantages. The disadvantages are studied and we find a new method which can almost obviate the most of these disadvantages. The new method is based on moment. It exploits the time delay, Doppler, and noise effects exerted onto the moments of the received data. The insight on the moments of the received signal is the criteria for joint estimation of time delay and Doppler. Since the moments of the noise could be obtained, these moments can facilitate separating the main signal from the noise even in a severe noisy environment. So, our estimation in low SNR has suitable results. In addition, we do not encounter with undesirable cross-terms discussed in WV method. After introducing our estimation method, its application in Doppler radar is declared.

The estimated delay and Doppler are used in the target tracking and predicting the position and velocity of the target in a noisy background. So it is applicable in the radar trackers. Test results provide a plausibility of the both estimations and tracking. The estimated position and velocity are completely accurate even in very low SNRs. The tracking can be extended to multiple targets. Based on the features described for mono-target tracking, it is expected to have acceptable results in multiple targets tracking. Multi tracking in low SNRs is one of the most important roles of a Doppler radar which is reachable based on the presented method.

8. References

[1] Bilik, I., Tabrikian, J., Cohen, A. (2006). "GMM-based target classification for ground surveillance Doppler radar," *IEEE Trans. on Aerospace and Electronic Systems*, vol. 42, no. 1, January.

[2] Bouchereau, F., Brady, D. (2008). "Method-of-moments parameter estimation for compound fading processes," *IEEE Trans. Comm.*, vol. 56, no. 2, pp. 166-172.

[3] Chassande-Mottin, E., Pai, A. (2005). "Discrete time and frequency Wigner-Ville distribution: Moyal's formula and aliasing," *IEEE Signal Processing Letters*, vol. 12, no. 7, pp. 508-511, July.

[4] Fukunaga, K., Flick, T. E. (1983). "Estimation of the parameters of a Gaussian mixture using the method of moments," *IEEE Trans. Pattern Analysis and Machine Intelligence*, vol. pami-5, no. 4, pp. 410-416, July.

[5] Gaeddert, J., Annamalai, A. (2005). "Some remarks on Nakagami-m parameter estimation using method of moments," *IEEE Comm. Letters*, vol. 9, no. 4, pp. 313-315.

[6] Greenstein, L. J., Michelson, D. G., Erceg, V. (1999). "Moment-method estimation of the Ricean K-factor," *IEEE Comm. Letters*, vol. 3, no. 6, pp. 175-176.

[7] Isaksson, A. J., Horch, A., Dumont, G. A. (2001). "Event-triggered deadtime estimation from closed-loop data," *In Proc. American Control Conf.*, Arlington, VA, USA, June.

[8] Jian, W., Yonggao, J., Dingzhang, D., Huachun, D., Taifan, Q. (2007). "Particle filter initialization in non-linear non-Gaussian radar target tracking," *Journal of Systems Engineerng and Electronics*, vol. 18, no. 3, pp. 491-496.

[9] Ma, X., Nikias, C. L. (1996). "Joint estimation of time delay and frequency delay in impulsive noise," *IEEE Trans. Signal Processing*, vol. 44, pp. 2669-2687, November.

[10] Niu, X., Ching, P., Chan, Y. (1999). "Wavelet based approach for joint time delay and Doppler stretch measurements," *IEEE Trans. on Aerospace and Electronic Systems*, vol. 35, no. 3, pp. 1111-1119.

[11] Orr, R. S., Morris, J. M., Qian, S. E. (1992). "Use of the Gabor representation for Wigner distribution crossterm suppression," *ICASSP-92*, vol.5, pp. 29-31, March.
[12] Park, S. T., Lee, J. G. (2001). "Improved Kalman filter design for three-dimensional radar tracking," *IEEE Trans. on Aerospace and Electronic Systems*, vol. 37, no. 2, pp. 727-739, April.
[13] Ristic, B., Arulampalam, S., Gordon, N. (2004). "Beyond the Kalman Filter: Particle filters for tracking applications," *Artech House*.
[14] Tan, J. L., Sha'ameri, A. Z. B. (2008). "Adaptive optimal kernel smooth-windowed wigner-ville for digital communication signal," *EURASIP Journal on Advances in Signal Processing*.
[15] Zabin, S. M., Wright, G. A. (1994). "Nonparametric density estimation and detection in impulsive interference channels. I. Estimators," *IEEE Trans. on Communications*, vol. 42, no. 2/3/4, pp. 1684-1697, February/March/April.

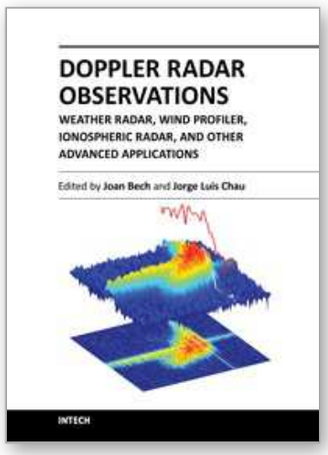

Doppler Radar Observations - Weather Radar, Wind Profiler, Ionospheric Radar, and Other Advanced Applications

Edited by Dr. Joan Bech

ISBN 978-953-51-0496-4
Hard cover, 470 pages
Publisher InTech
Published online 05, April, 2012
Published in print edition April, 2012

Doppler radar systems have been instrumental to improve our understanding and monitoring capabilities of phenomena taking place in the low, middle, and upper atmosphere. Weather radars, wind profilers, and incoherent and coherent scatter radars implementing Doppler techniques are now used routinely both in research and operational applications by scientists and practitioners. This book brings together a collection of eighteen essays by international leading authors devoted to different applications of ground based Doppler radars. Topics covered include, among others, severe weather surveillance, precipitation estimation and nowcasting, wind and turbulence retrievals, ionospheric radar and volcanological applications of Doppler radar. The book is ideally suited for graduate students looking for an introduction to the field or professionals intending to refresh or update their knowledge on Doppler radar applications.

INTECH
open science | open minds

InTech Europe
University Campus STeP Ri
Slavka Krautzeka 83/A
51000 Rijeka, Croatia
Phone: +385 (51) 770 447
Fax: +385 (51) 686 166
www.intechopen.com

InTech China
Unit 405, Office Block, Hotel Equatorial Shanghai
No.65, Yan An Road (West), Shanghai, 200040, China
中国上海市延安西路65号上海国际贵都大饭店办公楼405单元
Phone: +86-21-62489820
Fax: +86-21-62489821

IntechOpen